

A FERROELECTRIC FAST REACTIVE TUNER FOR SUPERCONDUCTING CAVITIES

N. Shipman*, J. Bastard, M. Coly, F. Gerigk, A. Macpherson, N. Stapley,
CERN, Geneva, Switzerland

I. Ben-Zvi, Brookhaven National Laboratory, Upton NY, USA

C. Jing, A. Kanareykin, Euclid Techlabs LLC, Gaithersburg MD, USA

G. Burt, A. Castilla, Lancaster University, Lancaster, UK

S. Kazakov, Fermi National Accelerator Laboratory, Batavia IL, USA

E. Nenasheva, Ceramics Ltd, St.Petersburg, Russia

Abstract

A prototype FerroElectric Fast Reactive Tuner (FE-FRT) for superconducting cavities has been developed, which allows the frequency to be controlled by application of a potential difference across a ferroelectric residing within the tuner. This technique has now become practically feasible due to the recent development of a new extremely low loss ferroelectric material. In a world first, CERN has tested the prototype FE-FRT with a superconducting cavity, and frequency tuning has been successfully demonstrated. This is a significant first step in the development of an entirely new class of tuner. These will allow electronic control of cavity frequencies, by a device operating at room temperature, within timescales that will allow active compensation of microphonics. For many applications this could eliminate the need to use over-coupled fundamental power couplers, thus significantly reducing RF amplifier power.

INTRODUCTION

Almost all RF cavities require some form of tuning in order to operate at the correct frequency. Superconducting cavities will often employ a mechanical tuner to correct large scale frequency deviations due to, for instance, He bath pressure fluctuations. However, mechanical tuners are generally too slow to correct fast frequency deviations from processes such as microphonics and dynamic Lorentz force detuning. Although progress is being made with 'fast' mechanical tuners employing piezo-electrics [1, 2], these present other difficulties such as the self-excitation of unwanted mechanical vibrations in the cavity affecting the frequency.

At present the most common way to overcome fast frequency shifts is to simply overcouple the fundamental power coupler in order to broaden the resonance. This is simple and effective but results in a large amount of wasted RF power. This is seen as particularly critical in ERLs and heavy ion accelerators where there is very little beam loading.

In this paper we present a new type of tuner, the FerroElectric Fast Reactive Tuner or FE-FRT. This new tuning method could offer frequency tuning orders of magnitude faster than what is currently available, with low losses, no moving parts, large tuning range and wide applicability across SRF.

* nicholas.shipman@cern.ch

HISTORY OF REACTIVE TUNERS

Reactive tuning is the controlled change of a cavity frequency by coupling to a tunable reactance. The control is electronic and no mechanical motion is needed so the change can be fast. Two types of reactive tuner already exist: pin diode based reactive tuners and ferrite based reactive tuners.

Pin diode based reactive tuners were first developed at CalTech in 1972 [3]. Later they were successfully used for several applications including: the ATLAS Linac in Argonne [4]; the Superconducting Proton Linac in Karlsruhe [5, 6]; and PIAVE at LNL-INFN [7, 8].

Pin diode tuners work by either shorting or leaving open a transmission line which is coupled to the cavity, presenting one of two possible reactances to the cavity. The average frequency of a cavity is controlled by adjusting the duty cycle between a high frequency and low frequency state. However, the RF frequency at which they can operate is usually limited due to the lumped nature of the diodes. The binary on-off switching also introduces phase ripple and modulating them at a high rate can be challenging.

Ferrite tuners have been studied since the mid 1950s, initially they were used to tune klystron cavities and were placed within the cavity structure [9]. They are now also used as the dielectric within a shorted co-axial transmission line coupled to a cavity [10]. Changing the biasing magnetic field of the ferrite changes its permeability and hence the electrical length of the transmission line. Varying the magnetic bias field thus alters the reactance seen by the cavity and so controls the frequency. Ferrite tuners typically suffer from fairly heavy losses particularly when operated below saturation or with biasing parallel to the RF magnetic field [11]. Their speed is limited by the difficulty in changing the current through the high inductance of the coil generating the magnetic field.

Ferroelectric phase and amplitude control was developed during the 1990's [12], in 2003 V. Yakovlev proposed RF switching by changing the frequency of a 'switching cavity' containing ferroelectric material [13]. In 2006 Ilan Ben-Zvi initiated FE-FRT research at BNL whereby the frequency of a cavity would be controlled by an external ferroelectric tuner. The first FE-FRT prototype was developed in 2011, but was never tested with an SRF cavity. Significant improvements

in the ferroelectric material have now been achieved and a new prototype has been tested with an SRF cavity at CERN.

THE FERROELECTRIC MATERIAL

Ferroelectrics have unique intrinsic properties that make them extremely attractive for high-energy accelerator applications. Their response time is $\approx 10^{-11}$ s for crystalline and $\approx 10^{-10}$ s for ceramic compounds. High dielectric breakdown strength, low gas permeability and easy mechanical treatment make ferroelectric ceramics promising candidates for the loading material in tuning and switching RF devices for accelerator applications. Typical representative ferroelectric materials are BaTiO_3 or a BaTiO_3 - SrTiO_3 solid solution (BST). The BST solid solution can be synthesized in the form of polycrystalline ceramic layers and in bulk [14–16].

Euclid Techlabs LLC have developed a BST(M) material [17] (BST ferroelectric with Mg-based additives) that allows fast switching and tuning in vacuum at a high biasing electric field of 50 kV/cm [18–20]. Initially this material was developed for the X-band frequency range [13, 21] (11.424 GHz) and demonstrated loss tangents of 5×10^{-3} at 10 GHz. Tunability, time response and loss factor measurements for large bulk ferroelectric samples have been presented and published recently [22].

A new BST-based material has been developed with a tunability of 6 – 8% at a 15 kV/cm biasing field to be applied in air [23–25]. Development of this type of material was a challenge; there are no other materials available with a tuning range and loss factor close to those listed above. It was demonstrated recently that by introducing a linear (non-tunable) Mg-based ceramic component into the BST solid solution one can enhance the tunability factor of the entire composition while keeping the loss tangent below 10^{-3} at L band [24, 25]. This counter-intuitive property (by increasing the non-tunable ceramic content of the ferroelectric-ceramic mixture one can enhance the tunability of the resulting material) opens important new possibilities in designing the specific class of microwave ceramic materials that will enable tuning at low magnitude biasing fields. In particular, an unprecedented low zero-field permittivity, non-linear material that retains tunability has been developed [23–25]: a BST ferroelectric and Mg-based additive composite with a dielectric constant in the range of ≈ 150 .

THEORY OF REACTIVE TUNING

Circuit Model

The equivalent circuit model of a cavity and reactive tuner system is shown in Fig. 1. We model the cavity as a conductance, capacitance and inductance, with values G_c , L_c and C_c respectively, connected in parallel. The cavity-tuner coupler is modelled as a lossless transformer of ratio N . The tuner, and the transmission line connecting it to the cavity, has an admittance Y'_t ; the real and imaginary parts of which are the conductance G'_t and susceptance B'_t respectively.

The cavity parameters Q_0 , R/Q and ω_0 can be calculated from the circuit element values G_c , L_c and C_c as follows [26]:

$$Q_0 = \frac{1}{G_c} \sqrt{\frac{C_c}{L_c}} \quad (1)$$

$$R/Q = 2 \sqrt{\frac{L_c}{C_c}} \quad (2)$$

$$\omega_0 = \frac{1}{\sqrt{L_c C_c}} \quad (3)$$

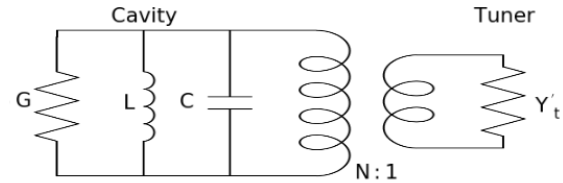


Figure 1: A parallel equivalent circuit representation of a cavity coupled to a reactive tuner. The transmission line is not shown but included in the value of Y'_t .

The tuner admittance as seen by the cavity is:

$$Y_t = G_t + iB_t = \frac{Y'_t}{N^2} \quad (4)$$

A prime is used to indicate a tuner quantity before it has been 'coupled into the cavity' through the transformer. In addition, where it is necessary to indicate that a quantity corresponds to a given tuner state¹, a subscript is used with 'n' denoting an arbitrary state and '1' and '2' being used to denote the 'end' states between which the maximum tuning range occurs. Y_{tn} for example would denote the admittance of the tuner, as seen by the cavity, in state 'n'.

Frequency Shift

The resonance of the cavity-tuner system, ω_n fulfils the condition:

$$\omega_n C_c - \frac{1}{\omega_n L_c} + B_t = 0 \quad (5)$$

After multiplying Eq. (5) through by $\omega_n L$, substituting in Eq. (2) and Eq. (3), defining the normalised frequency $\tilde{\omega}_n = \frac{\omega_n}{\omega_0}$, and re-arranging we get the following equation:

$$\tilde{\omega}_n = -\frac{B_t R/Q}{4} \pm \sqrt{1 + \left(\frac{B_t (R/Q)}{4}\right)^2} \quad (6)$$

As $\tilde{\omega}_n$ must be positive, we ignore the negative-sign solution in Eq. (6). Also, for small changes in frequency $\tilde{\omega}_n \approx 1$, therefore:

$$\left| \frac{B_t R/Q}{4} \right| \ll 1 \quad (7)$$

which implies:

$$\tilde{\omega}_n \approx 1 - \frac{B_t R/Q}{4} \quad (8)$$

¹ The state of an FE-FRT, for example, would be different for different voltages applied to it.

From Eq.(8) the maximum tuning range is therefore given by:

$$\Delta\omega_{12} = \frac{-\omega_0 \Delta B_{t12} R/Q}{4} \quad (9)$$

where $\Delta B_{t12} = B_{t2} - B_{t1}$. The size of the tuning can easily be made smaller or larger, by increasing or decreasing respectively, the size of the transformer ratio N . This is made clear by re-writing Eq. 9 as:

$$\Delta\omega_{12} = \frac{-\omega_0 \Delta B'_{t12} R/Q}{4N^2} \quad (10)$$

The tuning range also depends on the transmission line length as this affects $\Delta B'_{t12}$.

Power Dissipation and Bandwidth

The power dissipated by the tuner in state n is given by:

$$P_{in} = \frac{G_{tn} V_c^2}{2} \quad (11)$$

where V_c is the cavity voltage. We also know that the stored energy in the cavity U_c is given by:

$$U_c = \frac{C_c V_c^2}{2} \quad (12)$$

Using Eq. (11) and Eq. (12) we can eliminate V_c to obtain:

$$P_{in} = U_c \frac{G_{tn}}{C_c} \quad (13)$$

The reactive power \mathcal{P}_{in} is calculated in a similar fashion as:

$$\mathcal{P}_{in} = U_c \frac{B_{tn}}{C_c} \quad (14)$$

From Eq. (2), Eq. (3), Eq. (8) and Eq. (14) it can be shown that for case where the tuning range is centred on ω_0 , the peak reactive power is given by:

$$\mathcal{P}_{t1} = \mathcal{P}_{t2} = U_c \Delta\omega_{12} \quad (15)$$

The increase in the bandwidth (in rad/s) of the cavity-tuner system due to the tuner in state n , ΔBW_n , can be written as:

$$\Delta BW_n = \frac{P_{in}}{U_c} \quad (16)$$

From Eq. 13 and Eq. 16 we can write:

$$\Delta BW_n = \frac{G'_{tn}}{N^2 C_c} \quad (17)$$

Like Eq. (10), Eq. (17) depends on the coupling ratio N as well as the line length connecting the tuner to the cavity.

State Ratio and Figure of Merit

We now define the 'State Ratio' or SR as the full tuning range divided by the increase in bandwidth in state 'n'.

$$SR_n = \frac{\Delta\omega_{12}}{\Delta BW_n} \quad (18)$$

Substituting Eq. (10) and Eq. (17) into Eq. (18) we obtain:

$$SR_n = \frac{\Delta B'_t}{2G'_{tn}} \quad (19)$$

From Eq. 19 and Eq. 4 we see the SR is independent of both N and the cavity parameters, but still a function of both the state and transmission line length. It is a useful quantity to calculate the increase in bandwidth for a given state from the tuning range.

Next we define the figure of merit FoM for the tuner as the geometric average of the SR of the two end states:

$$FoM = \sqrt{SR_1 \times SR_2} \quad (20)$$

By substituting Eq. (19) into Eq. (20) we obtain:

$$FoM = \sqrt{\frac{(\Delta B_t)^2}{4G_1 G_2}} \quad (21)$$

For the case of a practical tuner where the modulus of the tuner's reflection coefficients as seen by the cavity, Γ_1 and Γ_2 , are close to one it is shown in the Appendix that the FoM can be well approximated as:

$$FoM \approx \frac{2|\sin \frac{\Delta\theta_{12}}{2}|}{\sqrt{(1 - |\Gamma_1(l)|^2)(1 - |\Gamma_2(l)|^2)}} \quad (22)$$

where $\Delta\theta_{12}$ is the difference in phase between Γ_1 and Γ_2 , and:

$$|\Gamma_n(l)| = |\Gamma_n(0)|e^{-2\alpha l} \quad (23)$$

where l is the length of transmission line and α the real part of the propagation constant [27]. The FoM depends only on the tuner and losses in the transmission line which may be neglected if small. If the line length is chosen such that $SR_1 = SR_2$ and provided the tuner is not operated across the short position in the smith chart, the FoM directly relates $\Delta\omega_{12}$ with the maximum ΔBW_n .

Figure 2 (left) shows how SR_1 , SR_2 , and the FoM with and without losses (Eq. (21) and Eq. (22) respectively), would be related as a function of line length for an exemplar FE-FRT. Figure 2 (right) shows corresponding values of Γ_1 and Γ_2 .

PERLE CASE STUDY

A preliminary investigation of the application of an FE-FRT to the PERLE project is now presented. The aim is not to develop a complete design, but to use the RF principles developed in the previous section together with the ferroelectric material parameters to realistically estimate the performance benefits that could be achieved.

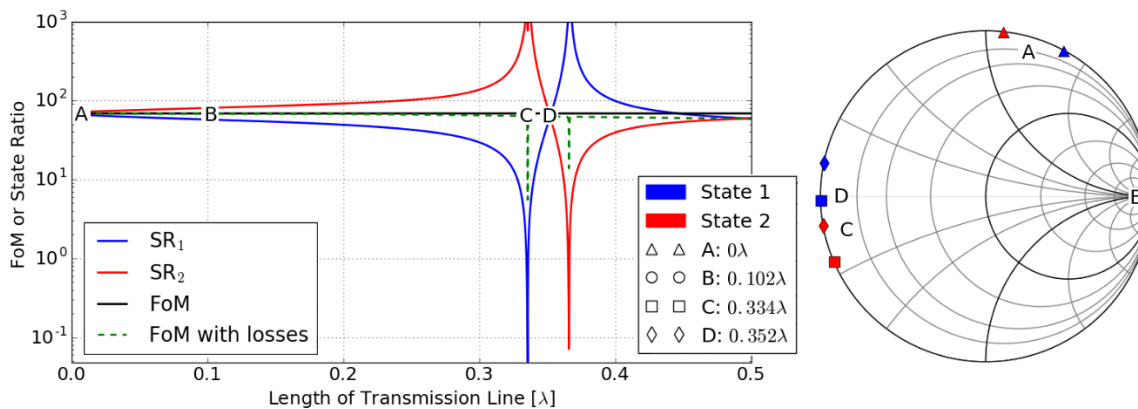


Figure 2: The theoretically derived relations between SR_1 , SR_2 and the FoM with and without losses for an exemplar FE-FRT model as a function of line length (left) and selected corresponding values of Γ_1 and Γ_2 (right).

The Powerful Energy Recovery Linacs for Experiments (PERLE) is a proposed energy recovery linac (ERL) aimed at developing and demonstrating ERL technology in the high energy, multi-turn and large beam current regime [28]. The cavity parameters are shown in Table 1.

Table 1: PERLE SC 5-cell Cavity Parameters

| Parameter | Value |
|---------------------|--------------------|
| ω_0 | 801.58 MHz |
| Q_0 | 2×10^{10} |
| R/Q | 393 Ω |
| U_c | 141 J |
| Q_{FPC} | 10^7 |
| P_{RF} | 45 kW |
| Max. Δf_μ | 40 Hz |

The RF cavities of an ERL typically have almost no beam loading. In this case, the RF power required to maintain the cavity voltage can be calculated from [29]:

$$P_{RF} = \frac{V_c^2}{4R/Q Q_L} \frac{\beta + 1}{\beta} \left[1 + \left(2Q_L \frac{\Delta\omega_\mu}{\omega_0} \right)^2 \right] \quad (24)$$

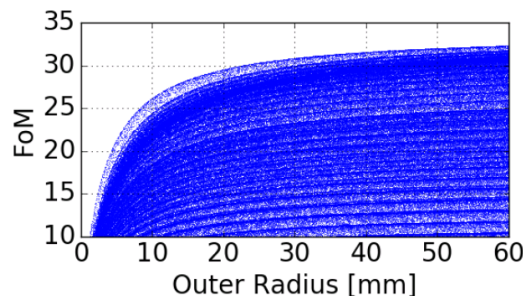
$\Delta\omega_\mu$, Q_L and β are the peak detuning, loaded Q and the fundamental power coupler's coupling parameter respectively. Equation (24) was used to infer the expected peak detuning, also shown in Table 1, from the Q_0 and Q_{FPC} specified in the PERLE CDR [28].

Table 2 shows the ferroelectric material parameters at 801.58 MHz and copper conductivity which were used in a co-axial transmission line model (TLM) of an FE-FRT to calculate the expected performance. A Monte Carlo method was used to estimate the physical dimensions which optimised the FoM, Fig. 3 shows these results for the outer diameter and length of the ferroelectric section.

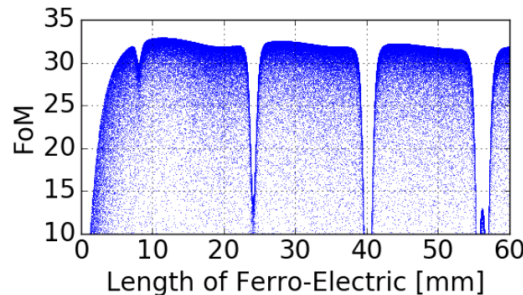
Once the optimum physical dimensions of the tuner model were found, the correct line length between the cavity and FE-FRT needed to be chosen. As the stored energy of the cavity

Table 2: Material Properties at 801.58 MHz

| Parameter | Value |
|------------------------------|-----------------------------------|
| Max. ϵ_r | 140 |
| Min. ϵ_r | 131.6 |
| $\tan \delta$ | 9.1×10^{-4} |
| $\frac{\Delta\epsilon_r}{E}$ | $0.6 \text{ kV}^{-1} \text{ cm}$ |
| σ_{Cu} | $5.96 \times 10^{-7} \text{ S/m}$ |



(a) The FoM vs. outer radius of ferroelectric section.



(b) The FoM vs. length of ferroelectric section.

Figure 3: Selected results of the Monte Carlo method applied to the physical dimensions of a co-axial TLM of an FE-FRT operating at 801.58 MHz.

is large we chose a line length with ω_0 in the centre of the tuning range in order to minimise the reactive power flowing in the tuner. Two such positions exist, roughly corresponding to, position 'B' and 'D' in Fig. 2, i.e. around the short

and open positions in the Smith chart. In this case it is not feasible to operate around the short position as the dissipated power in the tuner would increase enormously in the centre of the tuning range. Therefore the open position was chosen.

After including the additional dissipation from the correct length of transmission line the FoM was found to be approximately 30 from Eq. (21). With the correct line length in the TLM and given that the total tuning range must be twice the expected peak detuning, it was possible to calculate the transformer ratio from Eq. (10). The State Ratios, dissipated and reactive powers could then be calculated from Eq. (19), Eq. (13) and Eq. (14) respectively and are shown in Fig. 4.

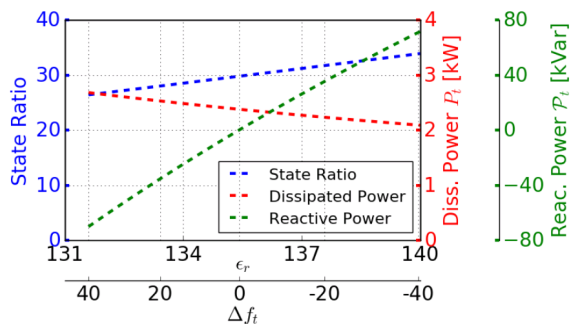


Figure 4: State ratio, dissipated and reactive powers as a function of ferroelectric permittivity and tuning.

Figure. 5 shows the dependence of the required forward power on the external Q of the fundamental power coupler with and without a tuner. The effect of a small residual detuning Δf_{res} caused, for example, by a non-perfect tuner control system is also shown and found to be negligible.

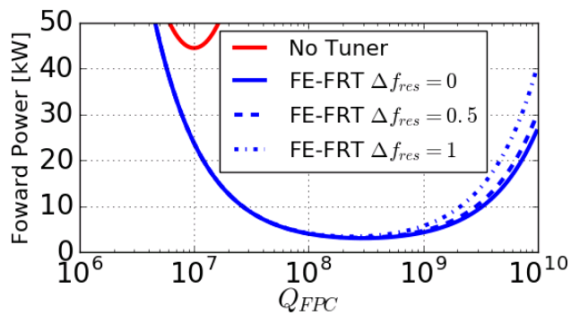


Figure 5: Dependence of forward power on the external Q of the fundamental power coupler for the PERLE 5-cell cavity with and without an FE-FRT. The effect of residual frequency detuning Δf_{μ} are also shown.

The expected tuner performance is summarised in Table 3. The peak RF power requirement is reduced by more than an order of magnitude to 3 kW. Due to the relatively high expected peak detuning and large stored energy of the cavity the power dissipated in the tuner itself, P_t is non-negligible and as part of a full design thermal simulations would need to be performed to consider how best to meet the cooling requirements. However, considering this power is dissipated at room temperature, even relatively small water coolers can easily provide the necessary cooling power.

Table 3: Properties of FE-FRT for PERLE

| Parameter | Value |
|----------------------|-----------------|
| FoM | 30 |
| Δf_t | 80 |
| Q_{FPC} | 3×10^8 |
| P_{RF} | 3 kW |
| P_t | 2.4 kW |
| Max. \mathcal{P}_t | 71 kVar |

Whilst this case study has already demonstrated the possibility of huge performance benefits, it should be noted that these are relatively conservative estimates. For example a permittivity tuning range of 6% was used but it is believed, that with careful tuner design to avoid high voltage breakdown, 8 – 10% could be achieved with no further material development. In addition the PERLE cavity operates at ≈ 800 MHz and the loss tangent is known to scale proportionally to the frequency over a wide range. The dielectric losses are therefore proportional to the square of the frequency as can be seen from Eq.(25) [27].

$$\alpha_d = 9.11 \times 10^{-8} f \sqrt{\epsilon_r} \tan \delta \quad (25)$$

FE-FRTs designed for cavities operating at lower frequencies therefore have the potential for even larger performance benefits. For a cavity operating at 100 – 200 MHz FoMs in the order of a few hundred are realistically achievable.

EXPERIMENTAL RESULTS

A prototype FE-FRT was built by Euclid and later acquired by CERN. The prototype FE-FRT together with a 3D rendering and simplified TLM are shown in Fig. 6. RF power from the cavity flows through the transmission line (T1) and into the left of the tuner (T2), through the ferroelectric material shown in light blue (T3) before being reflected by the RF short (T5). The high voltage bias is applied to the inner conductor at the right.

VNA measurements of the tuner made before and after brazing the ferroelectric to the outer and inner conductors revealed that the brazing significantly increased losses. These losses coupled with the long transmission line needed to reach the cavity positioned near the bottom of the ≈ 4 m deep cryostat significantly impaired the performance of the tuner. The tuner was tested with the UK 4-rod crab cavity [30] operating in it's lower order mode of ≈ 374 MHz. Unfortunately a super-fluid leak prevented cooling to 2 K. As such the antennas were not well coupled and limited transmitted signal was available reducing the signal to noise ratio of the frequency measurements. Nonetheless it was possible to both demonstrate frequency tuning and obtain an upper limit for the speed at which the tuner can operate.

Results of a TLM are compared to VNA measurements of the tuner and finite element analysis in Fig. 7. The agreement between the measured results and finite element analysis are

Content from this work may be used under the terms of the CC BY 3.0 licence (© 2019). Any distribution of this work must maintain attribution to the author(s), title of the work, publisher, and DOI.

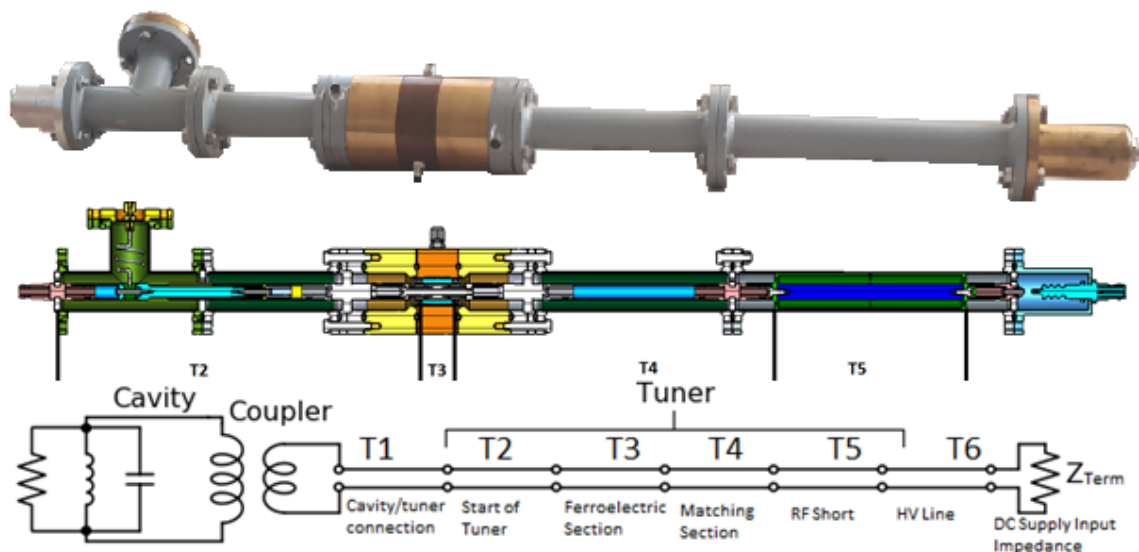


Figure 6: The equivalent circuit model used to model the FE-FRT and Cavity system compared to a cut-away rendering of the tuner. Corresponding transmission line segments have the same labelling.

close to perfect and the TLM results also show good agreement considering the many simplifications made, but why the resonance at ≈ 410 MHz predicted by the model is barely visible in the measured data needs further investigation.

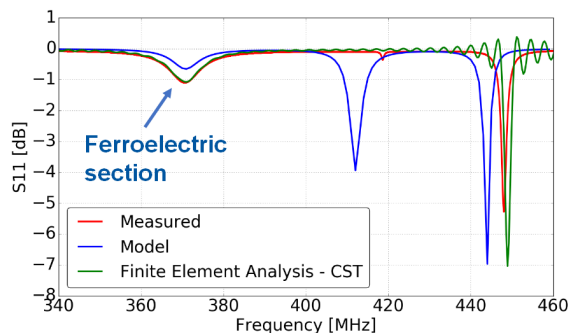


Figure 7: The magnitude of S11 against frequency: measured with the VNA (red); derived from a simplified TLM (blue); and calculated with CST Microwave Studio (green).

A simplified schematic diagram of the experimental setup is shown in Fig. 8. The cavity is placed in a cryostat and driven via a self excited loop (SEL). The FE-FRT is positioned vertically above the cavity and clamped to a mechanical stage allowing different lengths of cable to be inserted. A chiller is used to control the temperature of the FE-FRT and Nitrogen gas is inserted into the space between the inner and outer conductors to increase breakdown resistance. High voltage pulses can be applied to the FE-FRT by charging a bank of capacitors and closing a relay.

Three methods of recording the frequency were available: an analogue phase detection circuit read by an oscilloscope, a signal analyser (SA) and analysis of the transmitted I and Q signals recorded by the SEL. The first direct observations of tuning were made using the signal analyser and are shown in Fig. 9. The left most and right most red lines correspond

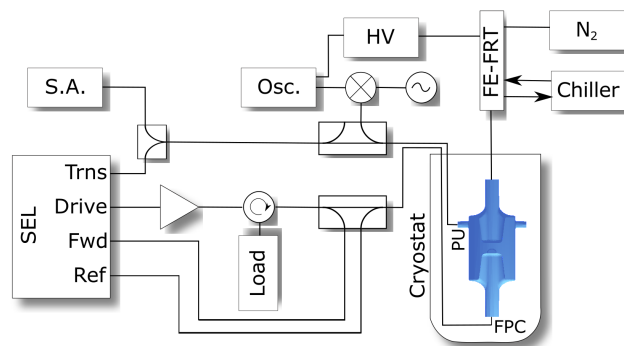


Figure 8: Schematic diagram of the experimental setup.

to the FE-FRT with 0 kV and 3 kV applied respectively. The drift of both lines from bottom right to top left is caused by slow fluctuations of the helium pressure inside the cryostat.

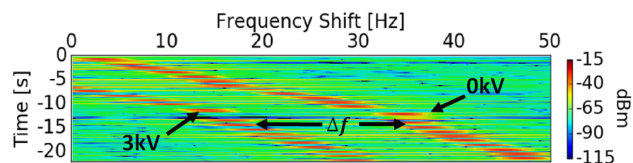


Figure 9: Direct observations of the frequency shift caused by the FE-FRT made with the signal analyser.

Figure 10 shows an example of the measured frequency whilst a high voltage pulse was applied. The frequency was calculated by converting the transmitted I and Q to phase and obtaining the gradient via linear regression. The 10 – 90 % fall time was calculated by fitting an error function.

Increasing the size of the regression window used to calculate the frequency reduces the error on the frequency measurement but decreases the time resolution, this is shown in

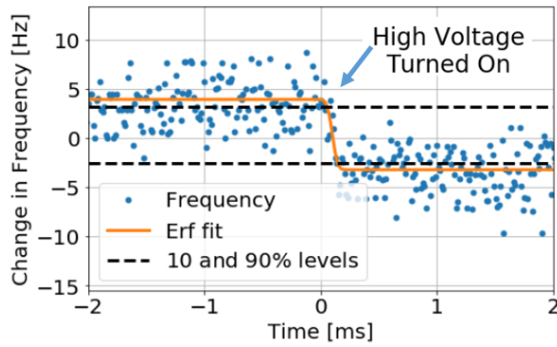


Figure 10: Measured frequency and fitted error function against time.

Fig. 11. When the window becomes too small it is no longer possible to accurately fit an error function to the data.

Brazing and transmission line losses decreased the loaded Q from 10^9 to $\approx 2 \times 10^7$. The cavity time constant was therefore ≈ 46 ms whilst the frequency shift occurred in $< \approx 50 \mu\text{s}$. It has therefore been shown that the timescale of the frequency shift for a reactive tuner is not limited by the time constant of the cavity.

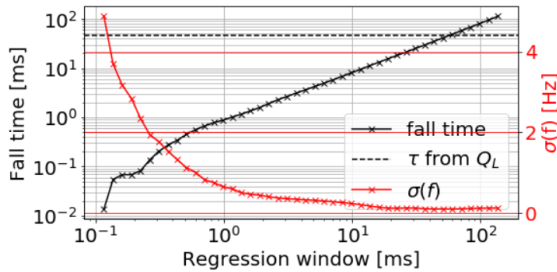


Figure 11: The dependence of the measured time of the frequency shift (black) and std. of the frequency (red) on the regression window.

A summary of the prototype FE-FRT performance is shown in Table 4. As already mentioned this was severely limited by both brazing and transmission line losses. Based on measurements of the ferroelectric material the next iteration of FE-FRT is expected to far exceed these numbers.

Table 4: Prototype FE-FRT Performance

| Parameter | Value |
|--------------------|-----------------|
| Δf_i | ≈ 12 Hz |
| ΔBW | ≈ 17 Hz |
| FoM | ≈ 0.7 |

CONCLUSION

The first ever FE-FRT test with a superconducting cavity has been performed and successfully demonstrated frequency tuning. The timescale in which the FE-FRT is able to shift the cavity frequency across the entire tuning range was

measured to be $< 50 \mu\text{s}$, this is significantly faster than any other cavity tuning device. This measurement was limited by the signal to noise ratio and the true timescale could well be more than an order of magnitude lower still. A maximum frequency tuning of ≈ 12 Hz was observed with an applied voltage of 3 kV, this could easily be increased by coupling more power to the tuner (see Eq.(10)).

Important contributions to the theory of FE-FRTs and reactive tuners in general have been made which allow a much deeper, and more intuitive, understanding of their behaviour. A case study of an FE-FRT applied to PERLE show RF power could be reduced by a factor of ≈ 15 .

APPENDIX

The Y'_{in} is related to Γ_n as shown below [31]:

$$Y'_{in}(z) = Y_0 \frac{1 - \Gamma_n(z)}{1 + \Gamma_n(z)} \quad (26)$$

Neglecting transmission line losses, the transformation of Γ with distance z along a transmission line is:

$$\Gamma(z) = \Gamma e^{2j\beta z} \quad (27)$$

We can thus define $\Gamma_n(z)$ as:

$$\Gamma_n(z) = |\Gamma_n| e^{j(2\beta z + \theta_n)} \quad (28)$$

From Eq. (26) and Eq. (28) we can obtain equations for G_n and B_n in terms of $|\Gamma_n|$ and θ_n :

$$G_n = Y_0 \frac{1 - |\Gamma_n|^2}{1 + 2|\Gamma_n| \cos(\tilde{z} + \theta_n) + |\Gamma_n|^2} \quad (29)$$

$$B_n = Y_0 \frac{-2|\Gamma_n| \sin(\tilde{z} + \theta_n)}{1 + 2|\Gamma_n| \cos(\tilde{z} + \theta_n) + |\Gamma_n|^2} \quad (30)$$

Substituting Eq. (29) and Eq. (30) in Eq. (21) we obtain after some algebra:

$$FoM = \sqrt{\frac{(2|\Gamma_1||\Gamma_2| \sin(\theta_1 - \theta_2) + J_{12} - J_{21})^2}{(1 - |\Gamma_1|^2)(1 - |\Gamma_2|^2)K_1K_2}} \quad (31)$$

with:

$$J_{nm} = |\Gamma_n|(1 + |\Gamma_m|^2) \sin(\tilde{z} + \theta_n) \quad (32)$$

$$K_n = 1 + |\Gamma_n|^2 + 2|\Gamma_n| \cos(\tilde{z} + \theta_n) \quad (33)$$

If $|\Gamma_1|$ and $|\Gamma_2|$ are close to one the FoM becomes:

$$\sqrt{\frac{(\sin(\theta_1 - \theta_2) + \sin(\tilde{z} + \theta_1) - \sin(\tilde{z} + \theta_2))^2}{(1 - |\Gamma_1|^2)(1 - |\Gamma_2|^2)L_1L_2}} \quad (34)$$

with:

$$L_n = (1 + \cos(\tilde{z} + \theta_n)) \quad (35)$$

After some algebra we obtain Eq. (36) as desired.

$$FoM = \frac{2|\sin \frac{\Delta\theta_{12}}{2}|}{\sqrt{(1 - |\Gamma_1|^2)(1 - |\Gamma_2|^2)}} \quad (36)$$

REFERENCES

- [1] S. Simrock *et al.*, “First Demonstration of Microphonic Control of a Superconducting Cavity with a Fast Piezoelectric TunerROAA004”, in *Proc. PAC’03*, Portland, OR, USA, May 2003, paper ROAA004, pp.470–472.
- [2] M. P. Kelly *et al.*, “A New Fast Tuning System for ATLAS Intensity Upgrade Cryomodule”, in *Proc. LINAC’10*, Tsukuba, Japan, Sep. 2010, paper THP057, pp. 884–886.
- [3] G. J. Dick and K. W. Shepard, in *Proc. 1972 Applied Superconductivity Conference*, Annapolis, Maryland, USA, May 1972, p. 649.
- [4] O. Despe, K. Johnson and T. Khoe, “Vibration-RF Control of Superconducting-Helix Resonators for Heavy-Ion Acceleration”, *IEEE Trans. Nucl. Sci.*, vol. 20 (3), p. 71, Jun. 1973. doi:10.1109/TNS.1973.4327046
- [5] D. Schulze *et al.*, “RF Control of Superconducting Helically Loaded Cavities”, in *Proc. 1972 Proton Linear Accelerator Conference*, Los Alamos, NM, USA, October 1972, G01, pp. 156–162. <http://accelconf.web.cern.ch/AccelConf/172/papers/g01.pdf>
- [6] G. Hochschild, D. Schulze and F. Spielböck, “Electronic Tuning and Phase Control of Superconducting Helical Resonators”, *IEEE Trans. Nucl. Sci.*, vol. 20 (3), p. 116, Jun. 1973. doi:10.1109/TNS.1973.4327057
- [7] V. Andreev, H. Ao and K. W. Shepard, “Design of the Fast Tuner Loop for Superconducting RFQs at INFN-LNL”, in *Proc. PAC’00*, Vienna, Austria, Jun. 2000, paper THP6B10, pp. 2013–2015.
- [8] G. Bassato *et al.*, “First Operation of PIAVE, the Heavy Ion Injector Based on Superconducting RFQ’s”, in *Proc. PAC’05*, Knoxville, TN, USA, May 2005, paper FPAE040, pp. 2621–2623.
- [9] G. Jones, J. Cacheris and C. Morrison, “Magnetic Tuning of Resonant Cavities and Wideband Frequency Modulation of Klystrons”, *Proc. IRE’56*, vol. 44, pp. 1431–1445, Oct. 1956. doi:10.1109/JRPROC.1956.274987
- [10] C. Vollinger and F. Caspers, “Ferrite-tuner Development for 80 MHz Single-Cell RF-Cavity Using Orthogonally Biased Garnets”, in *Proc. IPAC’15*, Richmond, VA, USA, May 2015, pp. 3159–3162. doi:10.18429/JACoW-IPAC2015-WEPHA023
- [11] L. Earley, G. Lawrence and J. Potter, “Rapidly Tuned Buncher Structure for the Los Alamos Proton Storage Ring (Psr)”, *IEEE Trans. Nucl. Sci.*, vol. 30, pp. 3511–3513, Aug. 1983. doi:10.1109/TNS.1983.4336708
- [12] R. Babbitt *et al.*, 1994. “Microwave Ferroelectric Phase Shifters and Methods for Fabricating the Same”, US Patent Office, US5334958A, Jul. 6, 1993.
- [13] V. Yakovlev *et al.*, “Ferroelectric Switch For An Active RF Pulse Compressor” *AIP Conf.Proc.* vol. 691, pp. 187–196. Dec. 2003. doi.org/10.1063/1.1635119
- [14] G. A. Smolensky, *Ferroelectrics and Related Materials*. New York, USA: Academic Press, 1981.
- [15] A. K. Tagantsev *et al.*, “Ferroelectric Materials for Microwave Tunable Applications”, *Journal of Electroceramics*, vol. 11, pp. 5–66, Sep. 2003. doi.org/10.1023/B:JECR.0000015661.81386.e6
- [16] O. G. Vendik *et al.*, “Ferroelectric Tuning of Planar and Bulk Microwave Devices”, *Journal of Superconductivity*, vol. 12 (2), pp. 325–338, Apr. 1999. doi.org/10.1023/A:1007797131173
- [17] E. Nenasheva and A. Kanareikin, 2011. “Low Dielectric Loss Ceramic Ferroelectric Composite Material”, US Patent Office, US8067324B2, Nov. 26, 2007.
- [18] E. A. Nenasheva *et al.*, “Ceramics Materials Based on (Ba, Sr)TiO₃ Solid Solutions for Tunable Microwave Devices”, *J. Electroceram.*, vol. 13, pp. 235–238, Jul. 2004. doi:10.1007/s10832-004-5104-0
- [19] S. F. Karmanenko *et al.*, “Frequency Dependence of Microwave Quality Factor of Doped Ba_xSr_{1-x}TiO₃ Ferroelectric Ceramics”, *Integrated Ferroelectrics*, vol. 61, pp. 177–181, Jan. 2004. DOI:10.1080/10584580490459332
- [20] A. Kanareykin *et al.*, “Tunable Ferroelectric Based Technologies for Accelerator Components”, in *Proc. EPAC’08*, Genoa, Italy, Jun. 2008, paper TUPPO46, pp. 1646–1648.
- [21] C. Jing *et al.*, “Experimental Demonstration of Wakefield Acceleration in a Tunable Dielectric Loaded Accelerating Structure”, *Phys. Rev. Lett.*, vol. 106, pp. 1–4, Apr. 2011. doi:10.1103/PhysRevLett.106.164802
- [22] S. Kazakov *et al.*, “Fast High-Power Microwave Ferroelectric Phase Shifters for Accelerator Application”, *AIP Conf.Proc.*, vol. 1086, pp. 477–484. Jan. 2009. doi.org/10.1063/1.3080953
- [23] E. Nenasheva *et al.*, “Low Loss Microwave Ferroelectric Ceramics for High Power Tunable Devices”, *Journal of European Ceramic Society*, vol. 30, pp. 395–400, Jan. 2010. doi:10.1016/j.jeurceramsoc.2009.04.008
- [24] A. Kozyrev *et al.*, “Observation of an Anomalous Correlation Between Permittivity and Tunability of a Doped (Ba,Sr)TiO₃ Ferroelectric Ceramic Developed for Microwave Applications”, *Appl.Phys. Lett.*, vol. 95, pp. 1–3, Jul. 2009. doi.org/10.1063/1.3168650
- [25] A. Kanareykin *et al.*, “Observation of an Anomalous Tuning Range of a Doped BST Ferroelectric Material Developed for Accelerator Applications”, in *Proc. IPAC’10*, Kyoto, Japan, May 2010, paper THPEB051, pp. 3987–3989.
- [26] H. Padamsee, “RF Superconductivity for Accelerators”. New York, NY, USA: Wiley, 1998.
- [27] T. Monero, “Microwave Transmission Design Data”, New York, NY, USA: Dover Pub. Inc., 1948.
- [28] D. Angal-Kalinin *et al.*, “PERLE. Powerful Energy Recovery Linac for Experiments. Conceptual Design Report”, *J. Phys. G: Nucl. Part. Phys.*, vol. 45, p. 065003, May 2018. doi:10.1088/1361-6471/aaa171
- [29] G. Hoffstaetter *et al.*, “Cornell Energy Recovery Linac: PDDR”, Ithaca, NY, USA, Cornell, Jun. 2013.
- [30] B. Hall *et al.*, “Design and testing of a four rod crab cavity for High Luminosity LHC”, *Phys. Rev. Spec. Top. Accel Beams*, vol. 20, p. 012001, Jan. 2018. doi:10.1103/PhysRevAccelBeams.20.012001
- [31] S. Silver, “Circuit Relations, Reciprocity Theorems”, in *Microwave Antenna Theory and Design*, Stevenage, UK: McGraw-Hill Book Comp. Inc., 1949, pp. 16–60.